Title: Multiscale dynamic mean field (MDMF) model to relate resting state brain dynamics with local cortical excitatory-inhibitory neurotransmitter homeostasis in health and disease.

Amit Naskar,[*1] Anirudh Vattikonda,[*1] Gustavo Deco[2], Dipanjan Roy[1#], Arpan Banerjee[# 1]

1. Cognitive Brain Dynamics Lab, National Brain Research Centre

NH 8, Manesar, Gurgaon 122052, India

2. Computational Neuroscience Research Group, Universitat Pompeu Fabra, Barcelona, Spain

#Email: arpan@nbrc.ac.in, dipanjan.nbrc@gov.in

(**Authors have equal contributions)*

Abstract

The spontaneous neuronal activity of human brain shows highly structured spatio-temporal pattern, designated as resting state network. Previous neuro-computational studies have established the connection of spontaneous resting state activity with neuronal ensembles (using dynamic mean field approach) and showed the impact of local inhibitory-excitatory balance on this patterned spontaneous resting state activity of brain. But, the role of neurotransmitter dynamics on large-scale network organization remains unexplored. Empirically, this is beyond the scope of current neuroimaging techniques to monitor the neurotransmitter changes and capture BOLD dynamics simultaneously. We argue that large-scale computational models offer an attractive platform to test out the possible neural mechanisms that operate at multiple scales of physiological organization namely, brain metabolism and changes in synaptic concentrations of GABA (gamma-aminobutyric acid)/ glutamate. We introduce a multiscale dynamic mean field (MDMF) model, that captures the synaptic gating dynamics as a function of neurotransmitter kinetics, we demonstrate how local homeostasis of excitatory-inhibitory neurotransmitter concentrations (GABA/ glutamate) could modulate the large-scale resting state network dynamics of brain. Simulations were carried out across glutamate (0.1 to 15 mmol) and GABA (0.1 to 15 mmol) concentration regimes that span the parameter space reported from healthy and diseased brains. We have found for optimal configurations of glutamate concentration ranging from 5.6 to 15 mmol and GABA concentration from 0.9 to 15 mmol model predicted functional connectivity matrix show closest match with empirical functional connectivity matrix of normal resting brain. Graph theoretical measures of segregation (modularity, clustering coefficient and local efficiency) and integration (global efficiency

and characteristic path length) in network information processing reported earlier in healthy and diseased brains were related to optimal GABA and glutamate concentrations and pathological values reported in epilepsy and schizophrenia respectively. In conclusion, the MDMF model could relate the various scales of observations from neurotransmitter concentrations to dynamics of synaptic gating to large-scale resting state network topology in healthy and in disordered states of the brain.

Key words: GABA, glutamate, resting-state functional connectivity, structural connectivity, network measures, epilepsy and schizophrenia.

Introduction

Exploration of human brain function is undertaken at different scales, from neurotransmitter modulations that controls the gating of ion channels and gives rise to membrane potential dynamics that leads to neuronal firing, and in turn get integrated across several thousands of neurons to generate characteristic spontaneous activity of brain areas. One of the most robust spontaneously generated spatiotemporal pattern of activity in distinct brain regions also called the resting state activity (Raichle and Mintun, 2006; Rogers et al., 2007; Vincent et al., 2007; Mitra et al., 2014) are observed in neuroimaging investigations when a human being is not instructed to undertake or follow specific instruction (task). Due to the simplistic nature of the task conditions or more precisely lack of task, has made this paradigm an important tool in studies of normal brain functions and in identifying markers for various neurological disorders (Pearlson, 2017; Zhou et al, 2017). Few studies have also attempted to understand the underlying mechanisms at the systems-level that govern the temporal dynamics of resting state networks (Deco & Jirsa, 2012; Deco et al., 2014a, Demirtas et al 2017, see also Cabral et al., 2017 for an overview).

All of these studies use neuro-computational models as a mechanism to link the spontaneous resting state activity to the dynamics of neuronal ensembles (more technically called the mean field activity) placed at different locations in cortex that are motivated by anatomical constraints obtained from tractography studies. Recent neuromodeling theories suggest that resting state correlations emerge when (i) the dynamic state of the brain is close to criticality i.e. at the edge of a bifurcation, and (ii) the excitatory inputs are balanced by local inhibitory processes maintain homeostasis (Deco & Jirsa, 2012; Deco et al., 2014a, Vattikonda et al., 2016). One important challenge is to understand how do the interaction of numerous

physiological parameter(s) like excitatory and inhibitory neurotransmitter concentration kinetics at the micro-scale level shapes up the spontaneous structured resting state dynamics of brain. The problem is further compounded by the fact that brain parameters, such as the proportion of different neurons and neurotransmitters types (glutamate, GABA etc.) with their association of synaptic properties cannot be manipulated independently in living system to delineate their role in brain function (Prinz, 2008). Due to these *in vivo* practical constraints, physiologically realistic whole brain network models are favorable candidates for the neuroscience community to overcome and manipulate experimentally inaccessible parameter(s) of neuronal networks in brain. Following this line of reasoning, mean field approach, consisting of coupled stochastic differential equations could provide appropriate neuro-computational framework to study missing link between micro-scale state variables with large-scale brain network dynamics (Breakspear et al., 2017).

Although, molecular, cellular and electrophysiological studies of neurons could show how post-synaptic neuronal response emerges depending on neurotransmitter types, yet its relation with global scale brain activity is not well addressed (Duncan et al., 2014). GABA and glutamate are the two key inhibitory and excitatory neurotransmitter respectively (Novotny et al., 2003) that are present all over the cortex (Duncan et al., 2014) and govern the excitatory-inhibitory (E/I) balance (Lauritzen et al., 2012). Applying statistical measures, several studies have demonstrated GABA has significant association with blood-oxygen-level dependent (BOLD) signal in health human brain (Northoff et al., 2010; Raichle et al., 2009). Moreover, interaction among inhibitory neurons and excitatory neurons is thought to have a direct influence on BOLD signal (Logothetis et al., 2001). In recent past, neuro-computational studies have shown how balance in local excitatory-inhibitory input involves

in spontaneous resting state activity in brain (Deco et al., 2014a; 2014b). Even, our group has shown importance of excitatory-inhibitory balance in view of functional recovery, e.g.- establishment of homeostasis over a re-organized brain network following a lesion in specific brain site (Vattikonda et al., 2016). As, imbalance in inhibition and excitation in brain is one of the key neuronal events involves in neurological disorders (Chiapponi et al., 2016), the study on GABA-glutamate balance would play a key role in exploring mechanistic insights of neurological diseases and its deviation from normal brain function.

In principle, a combination of fMRI-derived blood oxygen level dependent (BOLD) signal activity and magnetic resonance spectroscopy (MRS) techniques can be used to find out association of neurotransmitter concentration(s) and BOLD signal vis-a-vis resting state, but the major limitation is that fMRI and MRS cannot be conducted simultaneously (Hu et al., 2013). Hence, neurocomputational model as presented here provides a plausible link between rich resting state spatio-temporal dynamics in large-scale brain networks with underlying neurotransmitter concentration kinetics, which to the best of our knowledge has not been investigated before and thus remains as an open question. Here, we have used a kinetic equation to capture the the syanptic gating variable dynamics as a function of neurotransmitter concentration gradient. The excitatory and inhibitory currents in a given neural population/ network can be expressed as a function of synaptic gating vatiables summed over the entire field of neurons (Deco et al 2014b). In the current study, our model predicts that (i) homeostasis via E/I balance could be achieved only at a specific range of neurotransmitter concentrations, importantly close to concentrations reported in the literature from MRS measurements from healthy subjects (ii) any deviations from these optimal regimes can lead to a variety of pathological conditions such as epilepsy and

schizophrenia which we further verify based on multiple network measures of integration and segregation and finally our model is able to successfully reconcile a wide number of observations exist in the experimental findings.

Material and Methods

Generation of structural connectivity matrix. Our empirical data consist of T1 anatomical images collected from 49 healthy subjects (30 females, 19 males, mean age of 41.55 ±18.44) at Berlin Center for Advanced Imaging, Charite University Medicine, Berlin, Germany. In this pipeline, high-resolution T1 anatomical images are used to create segmentation and parcellation of cortical and subcortical grey matter. The empirical SC matrix of dataset used in this study is generated by using an automated pipeline (Schirner et al., 2015) for reconstruction of fibre tracks from T1 structural MR images and Diffusion-weighted images (DWI). Diffusion-Tensor-Imaging (TR 7500 ms, TE 86 ms, 61 transversal slices (2.0 mm), voxel size 2.3 × 2.3 × 2.3 mm, FoV 220 mm, 96 × 96 matrix) and GRE field mapping (TR 674 ms, TE1 5.09 ms, TE2 7.55 ms, 61 transversal slices (2.3 mm), were measured directly after the anatomical scans. The images obtained from these scans are used as input to the reconstruction pipeline to generate the SC matrix for each subject (Please refer to (Schirner et al., 2015) for a detailed outline of the pipeline for generating SC matrix). For each subject, binary white matter (WM) masks were used to restrict tracking to WM voxels. dw-MRI data are pre-processed using FREESURFER after extracting gradient vectors and values (known as b-table) using MRTrix. Upon extraction of gradient vectors and values using MRTrix, dw-MRI data are pre-processed using FREESURFER's Using the registration rule created by FREESURFER's function dt-recon we transform the high-resolution mask volumes from the anatomical space to the subjects diffusion space, which

will be used for fiber tracking. The cortical and subcortical parcellations contained in aparc+aseg.nii are resampled into diffusion space, one time using the original 1 mm isotropic voxel size (for subvoxel seeding) and one time matching that of our dw-MRI data, i.e., 2.3 mm isotropic voxel size. Based on that, a fractional anisotropy (FA) and an eigenvector map are computed and masked by the binary WM mask created previously. In order to improve existing methods for capacities estimation the approach makes use of several assumptions with regard to seed-ROI selection, tracking and aggregation of generated tracks (Schirner et al., 2015). Cortical gray matter parcellation of 34 cortical region of interest (ROI) in each hemisphere was undertaken following Desikan-Killiany parcellation (Deskan et al., 2006). To estimate connection strength (value range 0 to 1) between each pair of ROIs, probabilistic tractography algorithm is used to estimate how one ROI can influence other in cortical grey matter parcellation. Upon tractography the pipeline aggregates generated tracks to estimate structural connectome for each individual subject. The normalized weighted distinct connection counts used here contain only distinct connections between each pair of regions yielding a symmetric matrix.

Functional connectivity matrix. Resting state fMRI as well as corresponding diffusion weighted imaging (DWI) data were collected at the Berlin Centre for Advanced Imaging, Charité University, Berlin, Germany. The dataset consisted of structural connectivity - functional connectivity (SC-FC) pairs of 49 healthy subjects (30 females, 19 males, mean age of 41.55 ±18.44) used in this study. In summary, all the participants underwent resting state functional imaging (no task condition) with eyes closed for 22 minutes, using a 3T Siemens Trim Trio scanner and 12 channel siemens head coil (voxel size 3 × 3 × 3 mm). Each fMRI resting state data amount to a total of 661 whole brain scans (time points

recorded at TR=2s) were obtained during the resting state functional magnetic resonance imaging (rs-fMRI) session. Thus the blood oxygen level dependent (BOLD) time-series signal available for each participant has 661 time points aggregated across 68 regions of interest (ROIs) as per the Desikan-Killiany brain atlas (Desikan et al., 2006). The diffusion weighted tensors (TR=750 ms, voxel size 2.3 × 2.3 × 2.3 mm) computed from the dwMRI data recorded with 64 gradient directions were subjected to probabilistic tractography as implemented in MRTrix (Desikan et al., 2006) in order to obtain subject specific structural connectivity (SC). The major steps involved extracting BOLD signal from each ROI are Motion correction, brain extraction, high pass temporal filtering and six-degrees of freedom (DOF) linear registration to the MNI space. Each participant's functional images were registered to pre-processed T1-anatomical images and parcellated into 68 regions of interest (ROIs) using FREESURFER's Desikan- Killiany atlas (Desikan et al., 2006). In each of the 68 ROIs, representative BOLD signal is computed by calculating mean of BOLD signals from all the voxels in the corresponding ROI. Pairwise Pearson correlation coefficients were computed among ROI's from the z-transformed BOLD time-series to generate the resting state functional connectivity (rs-FC) matrix for each subject.

Computational model. Previous studies have shown that the dynamic mean field (DMF) approach (Deco et al, 2014a; Deco et al., 2014b) is able to capture the rs-FC from the empirical connections matrix extracted from the density of white matter fiber tracts connecting candidate brain areas. One can go further to identify the role of local excitatory-inhibitory homeostasis in shaping up rs-FC (Vattikonda et al., 2016). At the neurotransmitter level the kinetic model of receptor binding (Destexhe et al, 1994a; Destexhe et al, 1994b) relates the neurotransmitter concentration changes to the synaptic gating variable, We

propose that a multiscale model should be able to relate the neurotransmitter modulations to the rs-FC. The key link is the synaptic gating dynamics which is linked to neurotransmitter kinetics and further plays a lead role in generation of excitatory-inhibitory currents in a local population of neurons (mean field). We relate the mean field activity in an area to the BOLD activity by the haemodynamic model (Friston 2002, 2003). Hence, each cortical region is modeled as a pool of excitatory and inhibitory neurons with recurrent excitatory-excitatory, inhibitory-inhibitory, excitatory-inhibitory and inhibitory-excitatory connections, and coupled with neurotransmitters GABA and glutamate via NMDA (N-methyl-D-aspartate) and GABA synapses, respectively. Long-range connections are modeled as excitatory connections between excitatory pools of each region. Long-range inputs are also scaled according to normalized connection strength between regions derived from DTI. Here, excitatory population in an area receives following input currents: recurrent inhibitory currents, recurrent excitatory currents, long-range excitatory currents from excitatory populations in all other areas, as well as external currents.

Destexhe et al, 1994a; assumed that occurrence of neurotransmitter release at synaptic cleft can be considered a pulse following the arrival of an action potential at the presynaptic terminal. Thus, neurotransmitter release can be captured in the rate equation that describes the synaptic gating variable dynamics. The rate of change of synaptic gating variable can be expressed as neural response function (δ-spikes) scaled by normalized neurotransmitter concentration and the fraction of closed synaptic gating probability plus the contribution of leaky synaptic gating originating from fast processes. $R + T \rightleftarrows TR$

(1)

$$\frac{dS}{dt} = -\beta S + \alpha[T_{max}](1-S)\sum_{t_k}\delta(t-t_k) \quad (2)$$

Where, TR and R represents bound and unbound receptors, respectively. α and β are the forward and backward rate constants of binding of neurotransmitter on receptors. T_{max} is maximun neurotransmitter concentration. In Eq. 2, S represents the fraction of synaptic gating variable at open state. Thus, equations 1& 2 together describe evaluation of synaptic gating variable with time under the influence neurotransmitter concentration.

Based on the kinetic model of receptor binding (Destexhe et al, 1994a; Destexhe et al, 1994b), we have considered average release of glutamate (T_{glu}; concentration of glutamate) or GABA (T_{gaba}; concentration of GABA) in synaptic cleft is governed by firing rate of excitatory or inhibitory presynaptic neurons in an area i, and rate of synaptic gating is represented by equations Eq.7 and Eq.8 respectively.

Using DMF model (Deco et al, 2014a; Deco et al., 2014b) and kinetic model of receptor binding (Destexhe et al, 1994a; Destexhe et al, 1994b), we propose a MDMF in which each brain area, where dynamics of GABA synapses and excitatory NMDA synapses depend on GABA and glutamate concentration, respectively MDMF model is described by the following coupled nonlinear differential equations.

$$I_i^{(E)} = W_E I_0 + w_+ J_{NMDA} + G J_{NMDA} \sum_j C_{ij} S_j^{(E)} - J_i S_i^{(I)} \quad (3)$$

$$I_i^{(I)} = W_I I_0 + J_{NMDA} S_i^{(E)} - S_i^{(I)} \quad (4)$$

$$r_i^{(E)} = (a_E I_i^{(E)} - b_E)/(1 - exp^{(-d_E(a_E I_i^{(I)} - b_E)})) \quad (5)$$

$$r_i^{(I)} = (a_I\, I_i^{(I)} - b_I)/(1 - exp^{(-d_I(a_I I_i^{(I)} - b_I)})) \quad (6)$$

$$\frac{dS_i^E(t)}{dt} = -\beta^E S_i^E + \alpha^E(1 - S_i^E)T_{glu} r_i^E + \sigma v_i(t) \quad (7)$$

$$\frac{dS_i^I(t)}{dt} = -\beta^I S_i^I + \alpha^I(1 - S_i^I)T_{gaba} r_i^I + \sigma v_i(t) \quad (8)$$

Inhibitory plasticity rule (Hellyer et al, 2016)

$$\frac{dJ_i(t)}{dt} = \gamma r_i^I (r_i^E - \rho) \quad (9)$$

In this study, $I_i^{(E\ or\ I)}$, is denoted as input current to the area i, whereas superscripts I and E represents represent inhibitory and excitatory populations in area i. Population firing rate of excitatory and inhibitory populations of area are $r_i^{(E)}$ and $r_i^{(I)}$, respectively. $S_i^{(E)}$or $S_i^{(I)}$are average synaptic gating variable of area i. Effective external input, I_O is scaled by W_I and W_E for excitatory and inhibitory populations. Local feedback inhibitory coupling and excitatory coupling are J_i and J_{NMDA}, respectively. v_i in Eq. 7 and Eq. 8 is uncorrected standard Gaussian noise with amplitude of s = 0.001 nA. J_i denotes synaptic weight, in mean field it scales the strength of connection from inhibitory to excitatory sub-population within local population. Eq. 9, it describes the dynamics of J_i, which is inhibitory plasticity rule, changes in J_i (synaptic weight) to ensure that inhibitory current clamps the excitatory current of a population and thereby maintaining a homeostasis and G is global coupling factor in equation 3. Homeostasis is achieved with J_i dynamics such that firing rate of the excitatory population is maintained at a target-firing rate and chosen target-firing rate is the firing rate observed when the inhibitory and excitatory currents are matched. Target firing rate can be decided based on biophysical observations. Cij represents connectivity strength

of long range excitatory currents from the other areas to an excitatory population in area i. Subscript ij in C_{ij} denotes entry in structural connectivity matrix. Since, recurrent excitatory currents are already taken into account while computing the input current to an excitatory population all the diagonal elements, C_{ii} are set to zero in the SC matrix. Input currents to an inhibitory population in area i are as follows: re-current inhibitory currents, recurrent excitatory currents, and external currents. All parameters in model are set to same values as in Deco et al, 2014a; Deco et al., 2014b. Synaptic activity of each area is used as input to the hemodynamic model (Friston et al, 2000; Friston et al, 2003) to generate the resting-state BOLD responses of each brain area. Differential equations are solved numerically using Euler-Maruyama method with time step of 0.1 ms and all simulations are performed in MATLAB.

Network construction and graph analysis

Both negative and positive correlations are treated as connection weights by taking their absolute values. This absolute FC matrix is thresholded (0.05 to 0.4 with increments of 0.01) and finally, FC matrices thresholded with correlation value of 0.25 are used to binarize for the generation of multiple networks with various connection densities that are biologically plausible. Brain Connectivity Toolbox (BCT) is used to compute all the graph analytic measures that quantifies, segregation and integration in information processing among brain areas.

Integration measures:

(i) *Global efficiency:* Average inverse shortest path length in the network. Quantifies exchange of information across the whole network. It is inversely associated to the path

length; it indicates exchange of information across the entire network (Wang et al, 2010). Global efficiency of graph G is denoted by following formula: $E_{glob}\,(G) = \frac{1}{n(n-1)}\sum_{i\neq j\,\in G}\frac{1}{d_{ij}}$

where, i and j represent vertices in a graph, n is number of vertices and d_{ij} is the shortest path length between node i and node j in G.

(ii) *Characteristic Path Length:* Average shortest path length between all pairs of nodes in the network and measures efficiency of information transfer in a network.

Segregation measures:

(i) *Clustering coefficient* (C_p): C_p of a network is defined as the average of the clustering coefficients over all nodes in the network where the clustering coefficient C_i of a node i is calculated using following equation:

$$C(i) = 2E/k_i \times (k_i - 1)$$

where, E represents the number of exciting connections among the node $i's$ neighbors and k_i representing the degree of node i

(ii) *Local efficiency*, quantifies how well a network can exchange information when a node is removed

$$E_{local}\,(G) = \frac{1}{n}\sum_{i\in G} E_{glob}(G_i)$$

$E_{glob}(G_i)$ is the global efficiency of sub graph G_i, which is comprised of the neighbors of the node i

(iii) *Modularity*, quantifies the degree to which a network may be subdivided into clearly delineated groups

Q (modularity) = $1/4m \sum_{ij}(A_{ij} - \frac{k_i k_j}{2m}) s_i\, s_j$

If network contain n vertices, s_i & s_j are two groups for a particular division of the network, number of edges between vertices i and j is A_{ij} (values of A_{ij} are the elements of the adjacency matrix), k_i and k_j are the degree of nodes and m is the total number of the edges of the network.

Results

Whole-brain functional connectivity estimation

The architecture of the MDMF model, consisting of cortical areas or nodes interconnected with structural connectivity matrix is represented in Fig.1A. The large scale brain network (Fig.1B) with long-range excitatory projections among distributed brain areas contribute to resting brain activity. By construction the arrival of action potential in presynaptic terminal releases neurotransmitter in the synaptic cleft and it binds to the other side of cleft on receptors of post-synaptic membrane (inset image of Fig.1C). We make the assumption that released neurotransmitter at synaptic cleft appears as a pulse following arrival of an action potential at the presynaptic terminal. The total neurotransmitter release in synaptic cleft is modelled as the summation of δ-like spikes generated following arrival of action-potentials at the presynaptic terminal.

Each cortical area is described as pool of excitatory and inhibitory neurons with recurrent excitatory-excitatory, inhibitory-inhibitory, excitatory-inhibitory, and inhibitory-excitatory connection, whereas long range connections are modelled as excitatory connections between excitatory pools of each region (Fig.1C). Synaptic gating depends on neurotransmitter released in the synaptic cleft, hence average synaptic gating is governed with mean release of neurotransmitter in a node. So, the ensemble activity of each cortical area is the outcome of excitatory (E)-inhibitory (I) neurotransmitter homeostasis (Fig.1C). MDMF uses anatomical structural connectivity matrix to connect the distributed brain regions, following which dynamic-kinetic interactions (equations 3-9) generate BOLD signals in each parcellated brain region. Finally, functional connectivity matrix computed from simulated BOLD signal is matched with empirical FC (Fig.1D & E).

Steady state solutions of the MDMF model of resting brain

In Fig.2A & B, average synaptic gating of GABA or NMDA with population mean firing rate are represented by dotted line, generated by taking the steady state solutions for Eq. 7 and 8 of the MDMF model, whereas, the empty circles represent the gating kinetics of GABA or NMDA from the model proposed by Destexhe (1994b). We use fixed values of glutamate (7.46 mM) and GABA (1.82 mM) concentrations observed in precuneus of normal healthy individual's brain during resting state and reported in MRS study by Hu, et al, 2013). Fig.2 shows that in terms of average gating kinetics the MDMF model results at steady state are qualitatively equivalent to the model proposed by Destexhe (1994b).

Predicting the rs-FC from GABA-glutamate kinetics

We varied the glutamate and GABA concentrations from 0.1 to 15 mmol and solved equations 3-9 numerically. The difference in estimation between the empirical FC and model predicted FC across neurotransmitter concentration scenarios is measured using the Frobenius norm, as mentioned below:

$$FC\ distance = \sqrt{\sum_{i=1}^{N}\sum_{i=1}^{N} |FC\ Empirical(i,j) - FC\ Model(i,j)|^2}$$

Thus, *FC distance* quantifies the similarity/ distance between empirical and model predicted FC. We observed that glutamate concentration ranging from 5.6 to 15 mmol and GABA concentration from 0.9 to 15 mmol show high similarity between FC and model predicted FC, as depicted by the black region in Fig.3A. Empirical observations from MRS studies show that adult normal human brain contain glutamate from 6-12.5 mmol/kg and GABA from 1.3-1.9 mmol/kg (Govindaraju et al., 2000).

Further, we have investigated the relation of neuronal firing rate with neurotransmitter concentrations (0.1 to 15 mmol of glutamate or GABA). Low neuronal firing rate (~8 Hz, considered as stable) can be associated with the glutamate concentration ranging from 5.6 to 15 mmol and GABA concentration from 0.1 mmol to 15 mmol, as depicted in the black region in Fig.3B. High firing rate (>8 Hz) is considered as unstable, as it is shown red and yellow region of the Fig.3B.

Precuneus is identified as a key region of the resting brain and we have shown earlier that in-silico lesions to precuneus impact activity at distant regions of the cortex. A proof of concept validation of the MDMF model will be to explore if the seed-based whole brain connectivity with the precuneus as a seed can be predicted at least qualitatively. Seed based correlation in all parcellated regions with respect to precuneus is plotted in Fig 3C for empirical data, followed by similar maps computed from model data for low GABA (0.5 mmol) and glutamate (0.5 mmol; Fig.3D), in optimal GABA (1.3 mmol) and glutamate (7.8 mmol; Fig.3E) and for high GABA (14 mmol) and glutamate (14 mmol; Fig.3F) concentrations. The closest match to the empirical correlation map of normal individuals was identified for optimal GABA and glutamate conditions (Fig.3C, E).

Network analysis to evaluate the relationship between neurotransmitter concentration and the degree of functional segregation and integration

Previously, graph theoretical analysis of functional brain networks computed segregation and integration measures in epileptic (Wang et al., 2014; Yasuda et al., 2015; documented in table 3 & 4) and schizophrenia patients (Hadley et al., 2016; Ganella et al., 2017; documented in table 3 & 4) and showed disrupted topological properties as compared to healthy subjects. Further, empirical observations from epilepsy and schizophrenia patients

show dysfunction in glutamate-ergic or GABA-ergic neurotransmission plays key role in these disorders. Neurotransmitter concentration measured via MRS in these patients are tabulated in table 1 & 2. We computed the graph theoretical measures of functional segregation and integration using the Brain Connectivity Toolbox (BCT). Fig.4A, B, & C illustrate the network segregation measures, modularity, clustering coefficient, and local efficiency, respectively as a function of GABA and glutamate concentrations. All the segregation measures had minima for a regime of optimal GABA and glutamate values. An increase or decrease from these optimal values revealed a regime where all the segregation matrices increase considerably and can be related to pathological states of the brain. The shaded area in the figures captures the values of graph theoretic measures reported from healthy subjects along with the corresponding neurotransmitters (GABA and glutamate) concentration, whereas outside of the shaded region indicates pathological condition of brain. Interpretations from network segregation measures illustrate how low, medium or high GABA and glutamate concentration (Fig.4D-F) may lead to nodes of the underlying functional network to cluster together in aberrant conditions (Fig.4D, F) as compared to functional network in optimal glutamate-GABA ratios (Fig.4E).

Fig.5A, & B summarizes the outcome of applying network integration measures such as global efficiency and characteristic path length respectively across entire concentration range of GABA (0.1 to 15 mmol) and glutamate (0.1 to 15 mmol). Intuitively, characteristic path length is somewhat inverse of global efficiency, as we observe in Fig.5. Analogous to the segregation measures, the global efficiency peaks at optimal values of GABA and glutamate. Interestingly the regime of GABA and glutamate that were optimal was identical to the segregation measures in Fig.4. The shaded region represents graph theoretic measures

of healthy subjects along with the corresponding neurotransmitters (GABA and glutamate) concentration, whereas outside of the shaded region indicates parameter regimes reported for pathological brain states, e.g., epilepsy (Wang et al., 2014; Yasuda et al., 2015) , schizophrenia (Sun et al., 2016; Ganella et al., 2017). Nodes of a putative functional network tend to cluster together both in low (Fig.4D), or high GABA and glutamate (Fig.4F) state, thus the average distance along shortest path length between a node and other nodes of the functional network increases in these extreme scenarios. For instance, distance between two nodes (represented in green color, Fig.4D-F) is shown to be increased in abnormal condition (low or high GABA and glutamate). In contrast global efficiency decreases, as the nodes become closer in low or high GABA and glutamate state as compared to optimal GABA and glutamate condition (Fig.4E).

Discussion

In the present study, we have explained the large scale resting-state network dynamics of human brain as a function of excitatory and inhibitory neurotransmitter kinetics via the multiscale dynamic mean field (MDMF) model. In other words, it is an effort to bridge two different scales -neurotransmitter concentration kinetics and synaptic activation dynamics. Our model differs substantially in many ways from previously proposed dynamic mean field (DMF) model with local E/I balance introduced by Deco et al, (2014a). MDMF brings specificity to precisely quantify the role of the underlying neurotransmitter concentrations in measurable units from MRS, thus, opening up possibility of tracking departures from healthy to pathological brain states in a systematic manner.

In the following, we outline the most crucial findings from the current study, (a) there exist a regime of optimal balance between neurotransmitter (GABA/ glutamate) concentrations in the parameter space, where simulated functional connectivity (FC) accurately fits empirical FC, (b) a local homeostasis between neurotransmitter concentration could be achieved only at the precise range of GABA/ glutamate concentrations, importantly the value close to neurotransmitter concentrations derived from empirical MRS value of metabolites in healthy subjects, (c) graph-theoretical analysis of network segregation (modularity, clustering coefficient and local efficiency) and integration measures (global efficiency, and characteristic path length) in the identified parameter space reconcile a wide number of contradictory empirical observations in a variety of pathological conditions.

In the MDMF model, FC emerges from the interaction of underlying anatomical connectivity and mean synaptic dynamics at the neural population level from individual brain areas (see figure 1). As shown in Fig.1, neuronal or synaptic dynamics in each areas is

further governed by the concentration kinetics of receptor binding at the specific neurotransmitter level. Hence, there are two distinct scales of observation and measurement which this model is successfully able to connect. Recent studies have further shown that good fit between empirical FC and simulated FC using whole brain computational model can be achieved over a robust parameter space and the proposed model further extends this line of reasoning to connect multiple scales which opens up new avenues in the domain of computational neuropsychiatry (Deco et al., 2014a; Hellyer et al., 2016; Vattikonda et al., 2016). Specifically, identification of an optimal excitatory-inhibitory neurotransmitter homeostasis regime is critical for understanding dynamical working point shift associated with mental and neurological disorders (Cabral et al., 2012a; Cabral et al., 2012b; Deco et al., 2014b). Thus, MDMF could be used as a computational connectomics tool by clinicians and neuroscientists apart for studying a variety of questions related to neuropsychiatric disorders. Usage of computational whole brain models in predicting seizure propagation has been recently highlighted by Proix et al, 2017. To validate the applicability of MDMF model in the diseased brain, we undertook an extensive literature research to identify the GABA/ glutamate values in mental and neurological disorders (see table 1 & 2) . Further we pooled the studies that have applied graph theoretic measures on functional connectivity metrics on functional brain imaging data. Interestingly, deviation from optimal neurotransmitter concentration leads to prediction of pathological brain network states using MDMF. Graph properties such as modularity, clustering coefficient, local efficiency, global efficiency, and characteristic path length computed from simulated FC, across all the neurotransmitter concentration values could decrease or increase depending on how far away from the optimal values are chosen for selected combination of GABA/ glutamate concentrations.

This further resulted in a close qualitative match between empirical reports of segregation and integration measures and that coming out of the MDMF model. Importantly, the MDMF model provides a global picture for the pathophysiology of neuropsychiatric and neurogenerative disorders, where the communication among brain areas are classified in terms of local and global measures, and their relationship with the underlying physiological mechanism at molecular level.

There exist couple of dissonant findings in epilepsy research that uses MRS measurements of GABA and glutamate. On one hand, some reports show decreased GABA levels (Petroff et al., 1995), whereas on other hand some reports reveal increased GABA level (Chowdhury et al., 2015; Hattingen et al., 2014) in epilepsy patients as compared to healthy subjects. Concurrently, network segregation measures (modularity, clustering coefficient and local efficiency; Pedersen et al., 2015; Yasuda et al., 2015) and integration measure such as characteristic path length (Wang et al., 2014) are reported to be increased in epileptic patients as compared to healthy subjects (see Table 3 & 4). The network analysis of simulated FCs from MDMF model could succesfully predict the increase in network segregation and integration (characteristic path length) measure in low or high GABA level, which is in accordance to empirical observations. Hence, the model has the potential to serve as a neurocomputational platform to explore the direct relationship between topological organization of network dynamics with neurotransmitters kinetics.

Additionally, in MDMF, inhibitory plasticity rule replaces feedback inhibition control (FIC) compared to the earlier models (Deco et al., 2014a; Vattikonda et al., 2016) regulating homeostatic E/I balance mechanism while operating in a realistic neurotransmitters concentration regimes. Our results demonstrate that even if inhibitory plasticity rule is

applied locally, it can affect globally, the large-scale brain dynamics. The local inhibitory plasticity rule in the large-scale brain network is biologically relevant for providing stabilization in a plastic network and regulating optimal information flow and noise correlation (Sprekeler et al, 2007; Vogels et al, 2011).

The important limitations in MDMF at the current stage is the non-incorporation of some finer details that are relevant for functional brain network dynamics. First, we have taken a fixed value of GABA/ Glutamate concentration over the entire brain commensurate with measurements from MRS using single-voxel spectroscopy. However, the concentrations of these neurotransmitters are variable across different areas which can be measured from positron emission tomography (PET) recordings (D'Hulst, et al. 2015). Nonetheless, a detailed analysis with GABA/ Glutamate values in individual brain areas contributing to resting state dynamics remains out of scope at this point due to lack of availability of detailed data but will be an interesting issue to resolve in future. Second, the structural connectivity (SC) matrix that is used in this study does not contain any subcortical brain areas which may crucially play a role of driver in sculpting much of the endogenous activity of the brain (Freyer et al., 2011). Third, communication and synchronization between brain areas are typically modulated by distant dependent conduction delays. To keep our findings tractable and to avoid complexity, delays are neglected in this model, which may serve as a critical ingredient for shaping up global brain dynamics, giving rise to phenomenon such as oscillations, complex spatiotemporal patterns, chaos and multi stability (Ghosh et al, 2008; Deco et al, 2009). Fourth, we have avoided incorporation of neuromodulatory effects in the MDMF model because the discussion is purely limited to relative small time window of resting state. However, incorporation of all these features are possible in the MDMF

framework in future. In fact the DMF component can be replaced with thalamocortical models (e.g Freyer et al., 2011) to address homeostasis in EEG/ MEG data in future computational studies.

In summary, we have characterized the homeostasis of glutamate-GABA concentration via a realistic large-scale neural model and explained the shift of the balance reported by empirical recordings of healthy and diseased brain. The MDMF model could link multiple scales of observations from neurotransmitter concentration kinetics to synaptic activation to macroscopic reorganization of resting state network topology in health and it's breakdown in disease. Interestingly, the identification of the pathological neurotransmitter concentration space also opens up novel future direction in the quest of identifying specific sets of biomarkers for characterizing progression from health to disease. Another potentially interesting direction for this approach could be task fMRI data that is far less traversed at this point. However, given that it is a bit unrealistic and challenging to acquire patients fMRI data particularly during task conditions therefore a future direction of this whole brain computational model could be geared more towards generating specific predictions during task conditions or perturbation with brain stimulations (tDCS, TMS) with a high degree of patient specificity. Virtual lesions can be introduced as outlined in Vattikonda et al, 2016 for identification of reorganization in the whole brain connectome as a function of neurotransmitter homeostasis. This remains a target for our future research.

Acknowledgements:

This study was supported by National Post Doctoral Fellowship (PDF/2016/000378) from Science and Engineering Research Board (Department of Science and Technology, Government of India) to AN, NBRC Core funds, Ramalingaswami Fellowships (Department

of Biotechnogy, Government of India) to DR (BT/RLF/Re-entry/07/2014) and AB (BT/RLF/Re-entry/31/2011) and Innovative Young Biotechnologist Award (IYBA) to AB (BT/07/IYBA/2013). AB also acknowledges the support of Centre of Excellence in Epilepsy and MEG. DR was also supported by SR/CSRI/21/2016 extramural grant from the Department of Science and Technology (DST) Ministry of Science and Technology, Government of India.

References

Breakspear, M., 2017. Dynamic models of large-scale brain activity. Nat. Neurosci. 20, 340–352.

Cabral, J., Hugues, E., Kringelbach, M.L., Deco, G., 2012a. Modeling the outcome of structural disconnection on resting-state functional connectivity. Neuroimage 62, 1342–53.

Cabral, J., Kringelbach, M., Deco, G., 2012b. Functional Graph Alterations in Schizophrenia: A Result from a Global Anatomic Decoupling? Pharmacopsychiatry 45, S57–S64.

Cabral, J., Kringelbach, M.L., Deco, G., 2017. Functional connectivity dynamically evolves on multiple time-scales over a static structural connectome: Models and mechanisms. Neuroimage 160, 84–96.

Chiapponi, C., Piras, F., Piras, F., Caltagirone, C., Spalletta, G., 2016. GABA System in Schizophrenia and Mood Disorders: A Mini Review on Third-Generation Imaging Studies. Front. Psychiatry 7, 61.

Chowdhury, F.A., O'Gorman, R.L., Nashef, L., Elwes, R.D., Edden, R.A., Murdoch, J.B., Barker, G.J., Richardson, M.P., 2015. Investigation of glutamine and GABA levels in patients with idiopathic generalized epilepsy using MEGAPRESS. J. Magn. Reson. Imaging 41, 694–9.

D'Hulst, C., Heulens, I., Van der Aa, N., Goffin, K., Koole, M., Porke, K., Van De Velde, M., Rooms, L., Van Paesschen, W., Van Esch, H., Van Laere, K., Kooy, R.F., 2015. Positron Emission Tomography (PET) Quantification of GABAA Receptors in the Brain of Fragile X Patients. PLoS One 10, e0131486.

Deco, G., Jirsa, V., McIntosh, A.R., Sporns, O., Kötter, R., 2009. Key role of coupling, delay, and noise in resting brain fluctuations. Proc. Natl. Acad. Sci. U. S. A. 106, 10302–7.

Deco, G., Jirsa, V.K., 2012. Ongoing cortical activity at rest: criticality, multistability, and ghost attractors. J. Neurosci. 32, 3366–75.

Deco, G., Ponce-Alvarez, A., Hagmann, P., Romani, G.L., Mantini, D., Corbetta, M., 2014a. How Local Excitation-Inhibition Ratio Impacts the Whole Brain Dynamics. J. Neurosci. 34, 7886–7898.

Deco, G., McIntosh, A.R., Shen, K., Hutchison, R.M., Menon, R.S., Everling, S., Hagmann, P., Jirsa, V.K., 2014b. Identification of optimal structural connectivity using functional connectivity and neural modeling. J. Neurosci. 34, 7910–6.

Demirtaş, M., Falcon, C., Tucholka, A., Gispert, J.D., Molinuevo, J.L., Deco, G., 2017. A whole-brain computational modeling approach to explain the alterations in resting-state functional connectivity during progression of Alzheimer's disease. NeuroImage. Clin.

16, 343–354.

Desikan, R.S., Ségonne, F., Fischl, B., Quinn, B.T., Dickerson, B.C., Blacker, D., Buckner, R.L., Dale, A.M., Maguire, R.P., Hyman, B.T., Albert, M.S., Killiany, R.J., 2006. An automated labeling system for subdividing the human cerebral cortex on MRI scans into gyral based regions of interest. Neuroimage 31, 968–80.

Destexhe, A., Mainen, Z.F., Sejnowski, T.J., 1994a. An Efficient Method for Computing Synaptic Conductances Based on a Kinetic Model of Receptor Binding. Neural Comput. 6, 14–18.

Destexhe, A., Mainen, Z.F., Sejnowski, T.J., 1994b. Synthesis of models for excitable membranes, synaptic transmission and neuromodulation using a common kinetic formalism. J. Comput. Neurosci. 1, 195–230.

Duncan, N.W., Wiebking, C., Northoff, G., 2014. Associations of regional GABA and glutamate with intrinsic and extrinsic neural activity in humans—A review of multimodal imaging studies. Neurosci. Biobehav. Rev. 47, 36–52.

Freyer, F., Roberts, J.A., Becker, R., Robinson, P.A., Ritter, P., Breakspear, M., 2011. Biophysical mechanisms of multistability in resting-state cortical rhythms. J. Neurosci. 31, 6353–61.

Friston, K.J., Harrison, L., Penny, W., 2003. Dynamic causal modelling. Neuroimage 19, 1273–302.

Friston, K.J., Mechelli, A., Turner, R., Price, C.J., 2000. Nonlinear Responses in fMRI: The Balloon Model, Volterra Kernels, and Other Hemodynamics. Neuroimage 12, 466–477.

Ganella, E.P., Bartholomeusz, C.F., Seguin, C., Whittle, S., Bousman, C., Phassouliotis, C., Everall, I., Pantelis, C., Zalesky, A., 2017. Functional brain networks in treatment-resistant schizophrenia. Schizophr. Res. 184, 73–81.

Ghosh, A., Rho, Y., McIntosh, A.R., Kötter, R., Jirsa, V.K., 2008. Noise during rest enables the exploration of the brain's dynamic repertoire. PLoS Comput. Biol. 4, e1000196.

Govindaraju, V., Young, K., Maudsley, A.A., 2000. Proton NMR chemical shifts and coupling constants for brain metabolites. NMR Biomed. 13, 129–53.

Hadley, J.A., Kraguljac, N.V., White, D.M., Ver Hoef, L., Tabora, J., Lahti, A.C., 2016. Change in brain network topology as a function of treatment response in schizophrenia: a longitudinal resting-state fMRI study using graph theory. NPJ Schizophr. 2, 16014.

Hattingen, E., Lückerath, C., Pellikan, S., Vronski, D., Roth, C., Knake, S., Kieslich, M., Pilatus, U., 2014. Frontal and thalamic changes of GABA concentration indicate dysfunction of thalamofrontal networks in juvenile myoclonic epilepsy. Epilepsia 55, 1030–1037.

Hellyer, P.J., Jachs, B., Clopath, C., Leech, R., 2016. Local inhibitory plasticity tunes macroscopic brain dynamics and allows the emergence of functional brain networks. Neuroimage 124, 85–95.

Hu, Y., Chen, X., Gu, H., Yang, Y., 2013. Resting-state glutamate and GABA concentrations predict task-induced deactivation in the default mode network. J. Neurosci. 33, 18566–73.

Jiang, W., Li, J., Chen, X., Ye, W., Zheng, J., 2017. Disrupted Structural and Functional Networks and Their Correlation with Alertness in Right Temporal Lobe Epilepsy: A

Graph Theory Study. Front. Neurol. 8, 179.

Lauritzen, M., Mathiesen, C., Schaefer, K., Thomsen, K.J., 2012. Neuronal inhibition and excitation, and the dichotomic control of brain hemodynamic and oxygen responses. Neuroimage 62, 1040–1050.

Logothetis, N.K., Pauls, J., Augath, M., Trinath, T., Oeltermann, A., 2001. Neurophysiological investigation of the basis of the fMRI signal. Nature 412, 150–157.

Mitra, A., Snyder, A.Z., Hacker, C.D., Raichle, M.E., 2014. Lag structure in resting-state fMRI. J. Neurophysiol. 111, 2374–91.

Northoff, G., Duncan, N.W., Hayes, D.J., 2010. The brain and its resting state activity--experimental and methodological implications. Prog. Neurobiol. 92, 593–600.

Novotny, E.J., Fulbright, R.K., Pearl, P.L., Gibson, K.M., Rothman, D.L., 2003. Magnetic resonance spectroscopy of neurotransmitters in human brain. Ann. Neurol. 54, S25–S31.

Pearlson, G.D., 2017. Applications of Resting State Functional MR Imaging to Neuropsychiatric Diseases. Neuroimaging Clin. N. Am. 27, 709–723.

Pedersen, M., Omidvarnia, A.H., Walz, J.M., Jackson, G.D., 2015. Increased segregation of brain networks in focal epilepsy: An fMRI graph theory finding. NeuroImage. Clin. 8, 536–42.

Petroff, O.A., Pleban, L.A., Spencer, D.D., 1995. Symbiosis between in vivo and in vitro NMR spectroscopy: the creatine, N-acetylaspartate, glutamate, and GABA content of the epileptic human brain. Magn. Reson. Imaging 13, 1197–211.

Prinz, A.A., 2008. Understanding epilepsy through network modeling. Proc. Natl. Acad. Sci. U. S. A. 105, 5953–4.

Proix, T., Bartolomei, F., Guye, M., Jirsa, V.K., 2017. Individual brain structure and modelling predict seizure propagation. Brain 140, 641–654.

Raichle, M.E., 2009. A Paradigm Shift in Functional Brain Imaging. J. Neurosci. 29, 12729–12734.

Raichle, M.E., Mintun, M.A., 2006. Brain work and brain imaging. Annu. Rev. Neurosci. 29, 449–476.

Rogers, B.P., Morgan, V.L., Newton, A.T., Gore, J.C., 2007. Assessing functional connectivity in the human brain by fMRI. Magn. Reson. Imaging 25, 1347–1357.

Schirner, M., Rothmeier, S., Jirsa, V.K., Mcintosh, A.R., Ritter, P., 2015. An automated pipeline for constructing personalized virtual brains from multimodal neuroimaging data. Neuroimage 117, 343–357.

Sun, Y., Chen, Y., Lee, R., Bezerianos, A., Collinson, S.L., Sim, K., 2016. Disruption of brain anatomical networks in schizophrenia: A longitudinal, diffusion tensor imaging based study. Schizophr. Res. 171, 149–157.

Thakkar, K.N., Rösler, L., Wijnen, J.P., Boer, V.O., Klomp, D.W.J., Cahn, W., Kahn, R.S., Neggers, S.F.W., 2017. 7T Proton Magnetic Resonance Spectroscopy of Gamma-Aminobutyric Acid, Glutamate, and Glutamine Reveals Altered Concentrations in Patients With Schizophrenia and Healthy Siblings. Biol. Psychiatry 81, 525–535.

Vattikonda, A., Surampudi, B.R., Banerjee, A., Deco, G., Roy, D., 2016. Does the

regulation of local excitation–inhibition balance aid in recovery of functional connectivity? A computational account.

Vincent, J.L., Patel, G.H., Fox, M.D., Snyder, A.Z., Baker, J.T., Van Essen, D.C., Zempel, J.M., Snyder, L.H., Corbetta, M., Raichle, M.E., 2007. Intrinsic functional architecture in the anaesthetized monkey brain. Nature 447, 83–6.

Vogels, T.P., Sprekeler, H., Zenke, F., Clopath, C., Gerstner, W., 2011. Inhibitory plasticity balances excitation and inhibition in sensory pathways and memory networks. Science 334, 1569–73.

Wang, J., Qiu, S., Xu, Y., Liu, Z., Wen, X., Hu, X., Zhang, R., Li, M., Wang, W., Huang, R., 2014. Graph theoretical analysis reveals disrupted topological properties of whole brain functional networks in temporal lobe epilepsy. Clin. Neurophysiol. 125, 1744–1756.

Wang, J., Zuo, X., He, Y., 2010. Graph-based network analysis of resting-state functional MRI. Front. Syst. Neurosci. 4, 16.

Yasuda, C.L., Chen, Z., Beltramini, G.C., Coan, A.C., Morita, M.E., Kubota, B., Bergo, F., Beaulieu, C., Cendes, F., Gross, D.W., 2015. Aberrant topological patterns of brain structural network in temporal lobe epilepsy. Epilepsia 56, 1992–2002.

Zhou, J., Liu, S., Ng, K.K., Wang, J., 2017. Applications of Resting-State Functional Connectivity to Neurodegenerative Disease. Neuroimaging Clin. N. Am. 27, 663–683.

Table 1. Comparison of GABA levels measured with brain MRS recordings from epileptic patients and healthy subjects reported in the literature.

SL. No.	*Neurotransmitter*	*Epileptic patients as compared to control*	*Brain region*	*Reference*
1.	GABA	Increased	Dorsolateral prefrontal cortex	Chowdhury et al., 2015
2.	GABA	Decreased	Occipital lobe	Petroff et al., 1995
3.	GABA	Increased	Frontal area	Hattingen et al., 2014

Table 2. Comparison of GABA/ Glutamate levels measured with brain MRS recordings from schizophrenia patients and healthy subjects reported in the literature.

SL. No	*Neurotransmitter*	*Schizophrenia patients as compared to control*	*Brain region*	*Reference*
1.	GABA	Decreased	Occipital cortex	Thakkar et al., 2017
2.	Glutamate	Decreased	Occipital cortex	Thakkar et al., 2017

Table 3. Network segregation measures reported in literature using human brain fMRI from epileptic and schizophrenia patients relative to healthy subject.

Sl. no.	*Network segregation measures of brain*	*Epileptic patients as compared to control*	*Reference*	*SZ patients as compared to control*	*Reference*

1.	Clustering coefficient	Increased	Yasuda et al., 2015; Jiang et al., 2017; Wang et al., 2014; Pedersen et al, 2015	Increased	Hadley et al., 2016
2.	Local efficiency	Increased	Yasuda et al., 2015; Pedersen et al, 2015	Increased	Ganella et al., 2017
3.	Modularity	Increased	Pedersen et al, 2015		

Table 4. Network integration measures reported in literature using human brain fMRI from chizophrenia and epileptic patients relative to healthy subjects (empirical observations)

Sl. no.	***Network integration measures of***	***Epileptic patients as compared to***	***Reference***	***SZ patients as compared***	***Reference***

	brain	***control***		***to control***	
1.	Characteristic path length	Increased	Wang et al., 2014	Increased	Sun et al., 2016
2.	Global efficiency	Decreased	Wang et al., 2014; Yasuda et al., 2015	Decreased	Hadley et al., 2016; Ganella et al., 2017

Table 5. Parameters used to simulate multiscale dynamic field model (MDMF) model

I_0	0.382 nA	α^E	0.072 $ms^{-1}mM^{-1}$
J_{NMDA}	0.1	β^E	0.0066 ms^{-1}
W_E	1.0	α^I	0.53 $ms^{-1}mM^{-1}$
W_I	0.74	β^I	0.18 ms^{-1}
w_+	1.4	σ	0.001 (nA)
a_I	615 (nC^{-1}1)	G	1
b_I	177 (Hz)	γ	1
d_I	0.087 (s)	ρ	3
a_E	310 (nC^{-1}1)	d_E	0.16 (s)
b_E	125 (Hz)		

Fig.1. Multiscale dynamic field model (MDMF) set up A. Averaged anatomical connectivity or structural connectivity matrix of healthy human brains. B. Large-scale brain network composed of interconnected nodes. C. Local networks, represented by nodes or cortical areas, each separate node consists of excitatory (purple color) and inhibitory (black color) neurons with recurrent inhibitory-inhibitory, excitatory-excitatory, inhibitory-excitatory, and excitatory-inhibitory connection, and all nodes are interconnected with long-range excitatory neurons (orange color line). Each brain area is represented as a pool of excitatory (E; green) and inhibitory (I, red) neurotransmitters. In inset image, presynaptic neuron releases neurotransmitter in the synaptic cleft, and it binds with postsynaptic receptors. D. Model generated FC matrix, and its fit or similarity with empirical FC (E).

Fig. 2. Comparison of MDMF model prediction of synaptic gating variables at steady state and the gating kinetics model proposed by Destexhe (1994b). Model-generated average (A) GABA or (B) NMDA synaptic gating as a function of population mean firing rate (dotted lines) closely approximate the model proposed by Destexhe (1994b) (lines with empty circles).

Fig. 3. FC distance and neuronal firing as a function of GABA and glutamate concentrations. (A) *FC Distance*: Black color region represents highly similar (low FC distance) and yellowish region depicts distant similarity (high FC distance) between empirical rs-FC and model-generated FC. GABA and glutamate concentration ranging from 0.1 to 15 mmol are which captures the biologically realistic parameter regime is used for simulations. (B) *Neuronal firing rate*: We consider high neuronal firing leads to instability for various neurotransmitter concentration scenarios. Stable region (black color) denotes low rate of neuronal firing (<8 Hz), and unstable region (red-yellow) region represents firing rate more than 8 Hz. Seed-based correlation maps with respect to precuneus plotted for different scenarios (C) empirical FC, and model-generated FCs in (D) low, (E) optimal, or (F) high GABA and glutamate concentrations.

Fig. 4. Surface plots showing the changes in network segregation measures such as, modularity (A), clustering coefficient (B), and local efficiency (C) across GABA and glutamate concentrations. The effect of changes in GABA concentration at discrete values of

glutamate concentrations (7 mmol, blue line; 10 mmol, red line; 13 mmol, yellow line) on network segregation measures including modularity, clustering coefficient, and local efficiency increase in low or high GABA and glutamate concentrations, except in the shaded region (lower panel of A-C). In schematic representation, nodes of functional network cluster together in both low (D) and high (F) level of GABA and glutamate state as compared to optimal (H) GABA and glutamate concentrations. Any two nodes are appeared as green color.

Fig.5. Surface plots showing the changes in network integration measures including global efficiency (A) and characteristic path length (B) at various GABA and glutamate concentrations. In lower panel, the effect of changes in GABA concentration at discrete values of glutamate (13 mmol, yellow line; 10 mmol, red line; 7 mmol, blue line) on network integration measures shows decrease in global efficiency at low or high GABA and glutamate concentrations except in the shaded region, whereas characteristic path length follows inverse of the global efficiency.

Fig.1

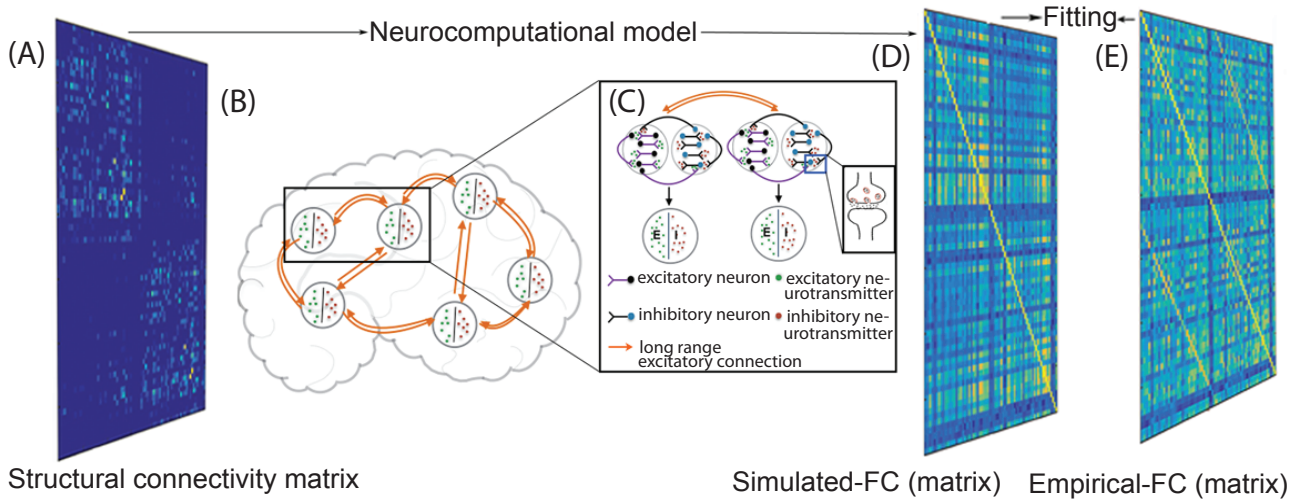
(A)
Neurocomputational model
(B)
(C)
(D)
Fitting
(E)
excitatory neuron
excitatory neurotransmitter
inhibitory neuron
inhibitory neurotransmitter
long range excitatory connection
Structural connectivity matrix
Simulated-FC (matrix)
Empirical-FC (matrix)

Fig.2

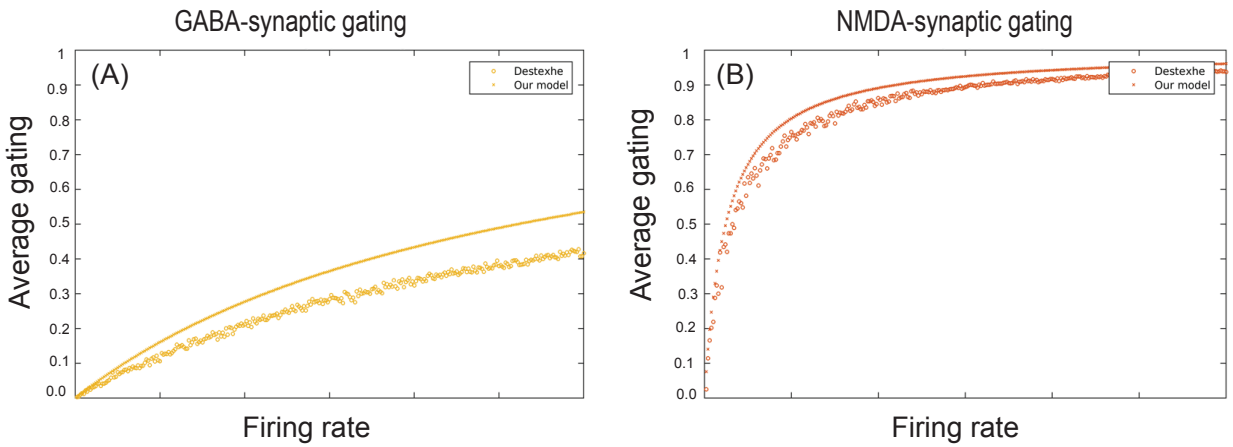
GABA-synaptic gating
(A)
Destexhe
Our model
Average gating
Firing rate
NMDA-synaptic gating
(B)
Destexhe
Our model
Average gating
Firing rate

Fig.3

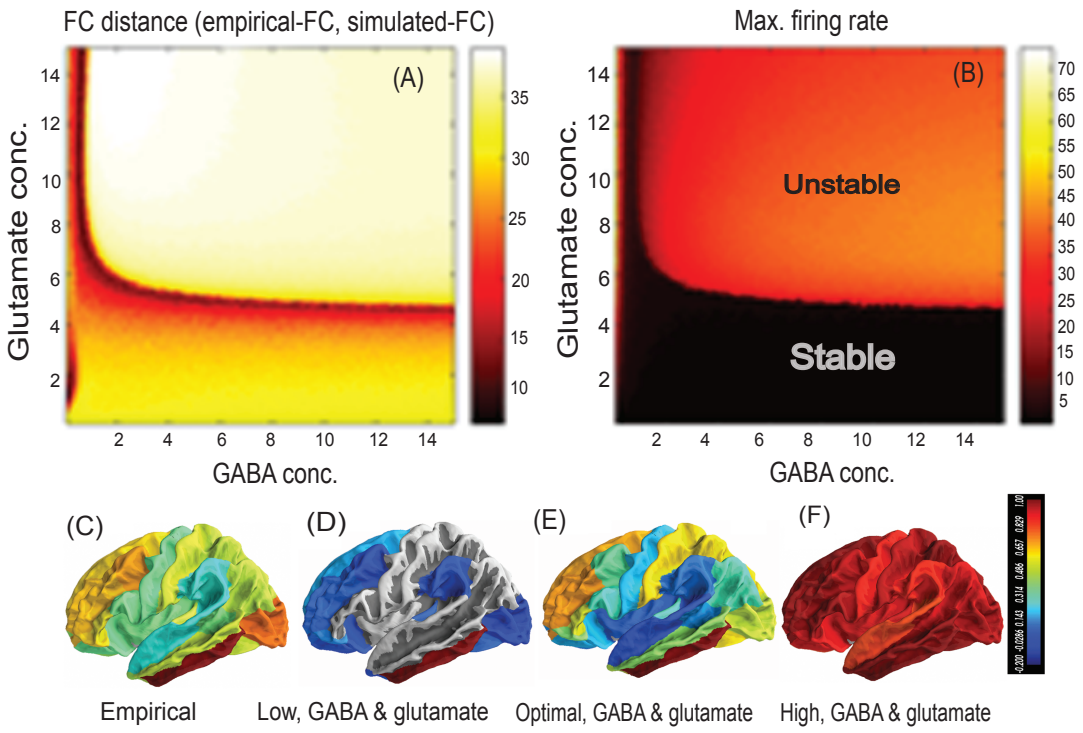
FC distance (empirical-FC, simulated-FC)
(A)
Glutamate conc.
GABA conc.
Max. firing rate
(B)
Unstable
Stable
Glutamate conc.
GABA conc.
(C)
(D)
(E)
(F)
Empirical
Low, GABA & glutamate
Optimal, GABA & glutamate
High, GABA & glutamate

Fig.4

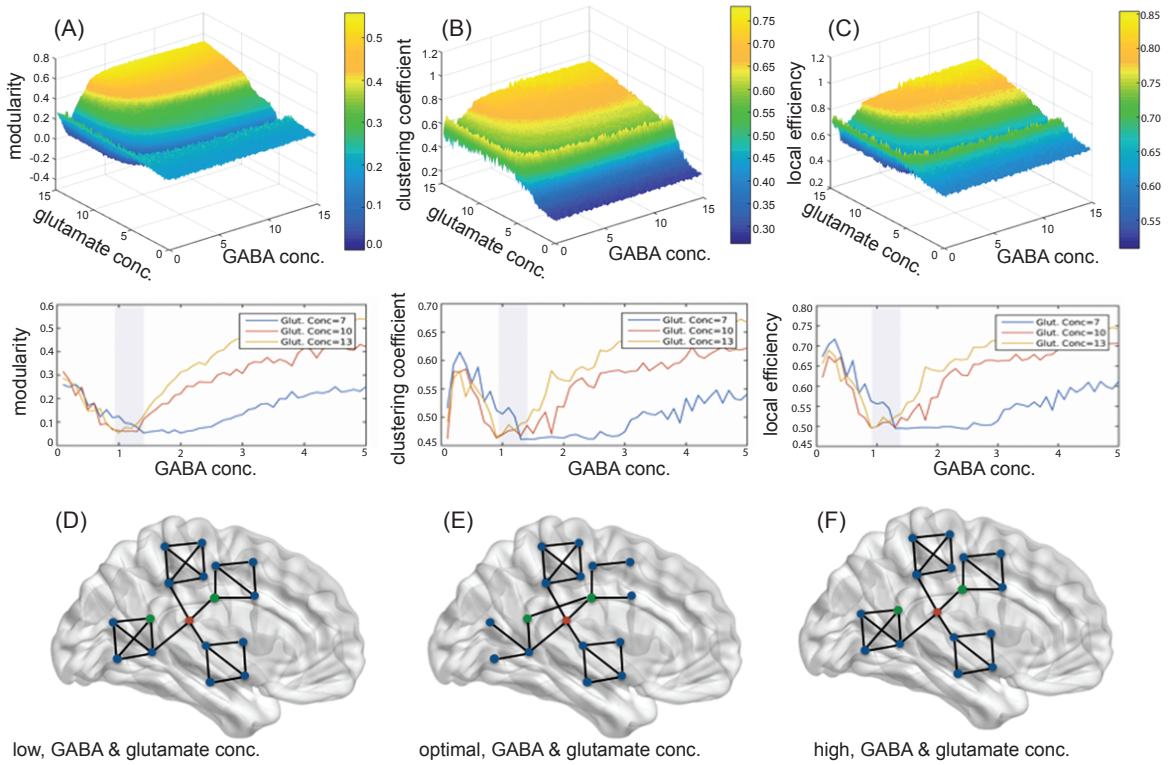
(A)
(B)
(C)
modularity
clustering coefficient
local efficiency
glutamate conc.
GABA conc.
Glut. Conc=7
Glut. Conc=10
Glut. Conc=13
(D)
(E)
(F)
low, GABA & glutamate conc.
optimal, GABA & glutamate conc.
high, GABA & glutamate conc.

Fig.5

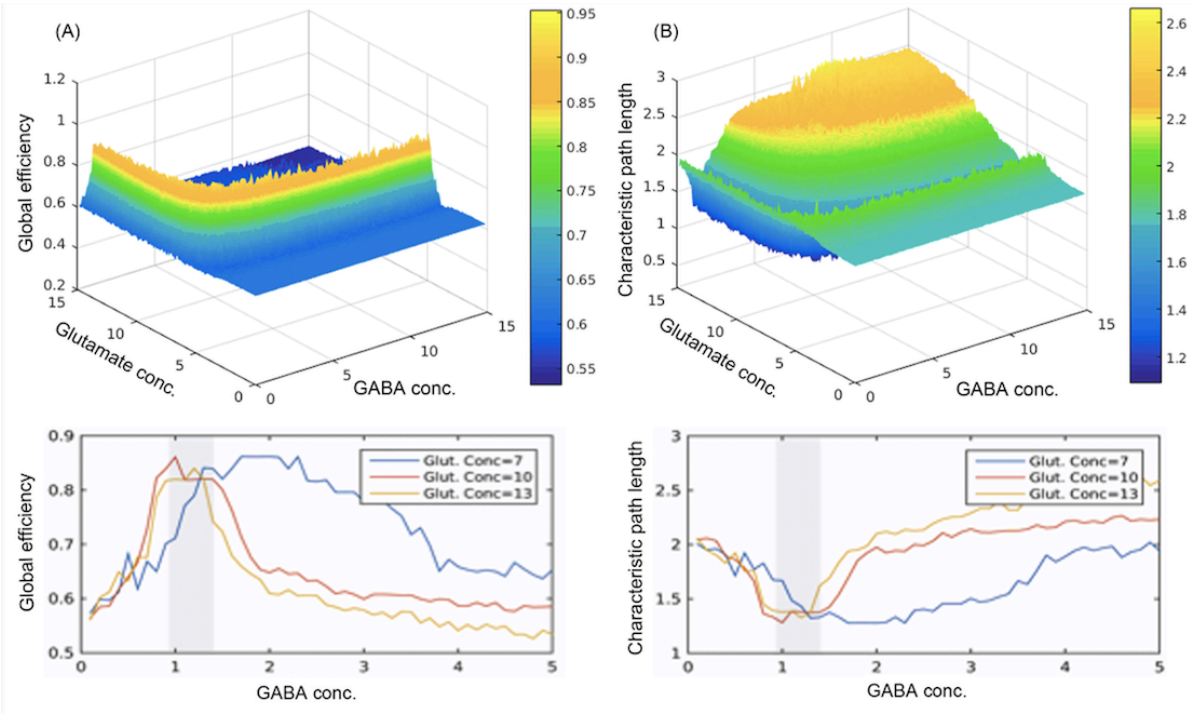
(A)
Global efficiency
Glutamate conc.
GABA conc.
(B)
Characteristic path length
Glutamate conc.
GABA conc.
Global efficiency
GABA conc.
Glut. Conc=7
Glut. Conc=10
Glut. Conc=13
Characteristic path length
GABA conc.
Glut. Conc=7
Glut. Conc=10
Glut. Conc=13